Smart Structures Systems, *Vol. 19, No. 4 (2017) 449-461*
DOI: https://doi.org/10.12989/sss.2017.19.4.449

A novel heuristic search algorithm for optimization with application to structural damage identification

Mehdi Nobahari[1], Mohammad Reza Ghasemi[*1] and Naser Shabakhty[2]

[1]*Department of Civil Engineering, University of Sistan and Baluchestan, Zahedan, Iran*
[2]*School of Civil Engineering, University of Science and Technology, Tehran, Iran*

(Received July 1, 2016, Revised December 19, 2016, Accepted February 24, 2017)

Abstract. One of the most recent methods of structural damage identification is using the difference between structures responses after and before damage occurrence. To do this one can formulate the damage detection problem as an inverse optimization problem where the extents of damage in each element are considered as the optimizations variables. To optimize the objective function, heuristic methods such as GA, PSO etc. are widely utilized. In this paper, inspired by animals such as bat, dolphin, oilbird, shrew etc. that use echolocation for finding food, a new and efficient method, called Echolocation Search Algorithm (ESA), is proposed to properly identify the site and extent of multiple damage cases in structural systems. Numerical results show that the proposed method can reliably determine the location and severity of multiple damage cases in structural systems.

Keywords: damage detection; modal frequency; inverse problem; optimization algorithm; echolocation search algorithm

1. Introduction

No matter how well they appear to have been designed, civil engineering structures can be damaged due to earthquake, storm, fire, corrosion or other issues during their service life. Such damages if not detected and amended early enough, they may lead to catastrophic structural failure. Therefore, detecting the position and extent of these damages is becoming increasingly important from both economic and life safety viewpoints. Finding the location and severity of these damages through local damage detecting methods such as visual inspection or localized experimental methods is not always possible. To overcome this difficulty, global damage detection (GDD) techniques are developed. The basic idea behind GDD is that a structural damage causes a decrease in the structural stiffness matrix that produces changes in the dynamic or static responses of the structure. A vibration based damage detection (VBDD) method as a GDD technique is based on changes in the modal properties (modal frequencies, mode shapes and modal damping) which has been widely utilized for structural damage identification.

A VBDD problem can be defined as an inverse problem that measured modal characteristics are used as inputs to determine damage locations and severities. The limited measured data of structure convert damage detection problem to an undetermined problem that have several solutions. Many methods have been introduced to solve this kind of inverse problems. One of the most general methods is based on employing optimization algorithms.

Maity and Tripathy (2005) used changes in modal frequencies for structural damage detection. They employed genetic algorithm to address the problem of damage detection. A nonclassical optimization approach involving the use of genetic algorithms (GAs) was proposed by Perera and Torres (2006) to localize damaged areas of the structure. The proposed method was based on the changes in frequencies and mode shapes of vibration of a structural system. He and Hwang (2006) combined an adaptive real-parameter genetic algorithm with simulated annealing to detect damage in beam-type structure. They used the displacements of the static response and natural frequencies of modal analysis as input data. Sahoo and Maity (2007) proposed a hybrid neuro-genetic algorithm. They used both natural frequencies and strains as input to determine the location and extent of structural damages. Begambre and Laier (2009) proposed a hybrid particle swarm optimization-simplex (PSOS) algorithm and considered frequency domain data as input parameters for structural damage identification. Sandesh and Shankar (2010) identified multiple crack damages in a thin plate using a novel heuristic search algorithm which was hybrid of particle swarm optimization (PSO) method and genetic algorithm (GA). Nobahari and Seyedpoor (2011) proposed an efficient correlation based index (ECBI) and a modified genetic algorithm to determine the site and severity of damages. Moradi *et al*. (2011) using the bees algorithm (BA) identified the crack location in beams. The objective function in their study was the weighted sum of the squared errors between the measured and computed natural frequencies. A two-step approach to multi-damage detection for plate structures was introduced by Xiang and Liang (2012). In the first step they focused on finding

*Corresponding author, Professor
E-mail: mrghasemi@hamoon.usb.ac.ir

ISSN: 1738-1584 (Print), 1738-1991 (Online)

damage location by applying the wavelet transformation. In the second step then damage events at the identified location are determined by using a PSO algorithm. Seyedpoor (2012) proposed a two stage method for identifying the site and extent of multiple damage cases in structures. In the first stage, using the concept of modal strain energy, located the eventual damage of structure. In the second stage, the extent of actual damage was determined via a particle swarm optimization (PSO) using the first stage results. An immunity enhanced particle swarm optimization (IEPSO) algorithm, which combines particle swarm optimization (PSO) with the artificial immune system, was proposed by Kang *et al*. (2012) for damage identification of structures. They used natural frequencies and mode shapes as input data in this study. Baghmisheh *et al*. (2012) formulated the identification of a crack location and depth in a cantilever beam as an optimization problem and solved this inverse problem by using a hybrid particle swarm-Nelder-Mead (PS-NM) algorithm. An improved charged system search (CSS) for damage detection of truss structures using changes in natural frequencies and mode shapes was proposed by Kaveh and Zholghadr (2015).

Among different structural responses that can be used as inputs for inverse structural damage identification problem, modal parameters (modal frequencies and mode shapes) are more attractive because they enjoy the benefit of being independent from excitation and can be measured conveniently. Also modal frequencies can be measured from just a few accessible points on the structure and are less vulnerable to experimental noise than mode shapes. Despite the fact that damage detection using only natural frequencies are very attractive, it is not possible to identify the location and extent of any damage by using only frequencies. In this paper we use the natural frequencies for structural damage identification.

Since 1950s that the idea of using evolution as an optimization tool for engineering problems was proposed, several heuristic search algorithms such as GA, PSO, ACO, DE etc. have been proposed. They have shown to be robust for solving various types of engineering problems and many engineers demonstrated their abilities in several different fields. Among those researchers one may refer to Wang and Ohmori (2013), Kang and Li (2015), Kaveh and Maniat (2015), Manoharan *et al*. (2015), Kang *et al*. (2016) and Seyedpoor and Montazer (2016).

Although heuristic search algorithms are a robust tool for structural damage identification, however they impose much computational cost to the damage detection process due to the stochastic base of these search algorithms. It is more considerable when there are a great numbers of structure elements and continues nature of damage variables is considered.

In this paper a novel search algorithm, Echolocation Search Algorithm (ESA), is proposed for structural damage identification using changes in modal frequencies. Considerable role of training for finding new situations in search space in proposed algorithm causes a significant decrease in required computational effort. In each iteration of a heuristic search algorithm such as GA, PSO etc., equal to the number of design points, analyses are carried out and corresponding to each design, its objective function is calculated. Each point according to its fitness will have a role in creating new points. Thus weak points may have little if any choice in creating new spots while there is a high chance for fitter ones to play the major role. In this case, the analysis cost for weak points may well be wasted.

The ESA diplomacy for generating new points is quite different compared to other such algorithms. In ESA, every point is a set of information, and is considered important. The fitness of each point, is only a data of this set of information. ESA, by comparing the information of all points (whether weak or strong) creates new points. For creating each new point, the information of three points are needed, therefore it is highly possible that the information of all points are used for generating new points. Numerical results show that proposed algorithm with high accuracy and efficiency can determine the site and severity of structural damages and can utilize it as a robust tool for optimization problems.

2. Problem formulation

When a damage event occurs, the stiffness of the damaged element is reduced. In many studies on structural damage detection, the damage has been simulated by decreasing one of the element's stiffness parameters, such as the moment of inertia, cross sectional area or elasticity modulus. In this paper, the damage of each element was simulated via the reduction of the elasticity modulus. To incorporate this, an elasticity modulus reduction factor x was introduced as follows

$$x_i = \frac{E - E_i}{E} \tag{1}$$

Where E is the initial elasticity modulus and E_i is the new elasticity modulus of the i^{th} element. Then if damage occurs in the i^{th} element, its stiffness matrix will be modified as

$$K_{d_i} = (1 - x_i)K_i \tag{2}$$

where $K_i$and $K_{d_i}$are initial and updated values of the i^{th} element stiffness matrix, respectively. Then structure's stiffness matrix is created by assembling the element stiffness matrices. In this work, the mass matrix change due to damage occurrence was ignored. Change in the structure's stiffness matrix leads to changes in natural frequencies. Determining the level of correlation between the measured and predicted modal responses (natural frequencies) can provide a simple statistical tool for finding the location and severity of structural damage. To do this, several objective functions have been proposed in the literature. In this paper, the efficient correlation based index (ECBI), as developed by Nobahari and Seyedpoor (2011), was used. This function merely considers the natural frequencies of the structure and is defined as

$$ECBI(X) = \frac{1}{2}(MDLAC(X) + obj(X)) \tag{3}$$

where *MDLAC(X)* is expressed in the following form

$$MDLAC(X) = \frac{|\Delta F.\delta F(X)|^2}{(\Delta F^T.\Delta F)(\delta F(X).\delta F(X))} \quad (4)$$

And $obj(X)$ is defined as

$$obj(X) = \frac{1}{nf}\sum_{1}^{nf}\frac{\min(f_{xi}, f_{di})}{\max(f_{xi}, f_{di})} \quad (5)$$

Also

$$\Delta F = \frac{F_h - F_d}{F_h} \quad (6)$$

And

$$\delta F(X) = \frac{F_h - F(X)}{F_h} \quad (7)$$

In the above relations, $X^T=\{x_1, x_2, x_3, ...,x_n\}$ represents a damage variable vector containing the damage severity (x_i, i=1, ..., n) of all n structural elements, $F(X)$ is a natural frequency vector that can be computed from an analytic model, F_h and F_d refer to the natural frequency vectors of healthy and damaged structures and finally, f_{x_i} and f_{d_i} are the i^{th} components of vectors $F(X)$ and F_d, respectively. For evaluating the $ECBI(X)$, only the first nf natural frequencies are considered.

The $ECBI(X)$ compares the change vector of measured and analytical frequencies. The $ECBI(X)$ varies from a minimum value of 0 to a maximum value of 1. It will be maximal when the analytical frequencies vector becomes identical to the frequency vector of the damaged structure, $F(X)=F_d$. Then damage detection problem can be solved by using an optimization algorithm to find a set of damage variables maximizing the $ECBI(X)$

$$\begin{aligned} &Find \quad X^T = \{x_1, x_2, \dots, x_n\} \\ &Maximize \quad ECBI(X) \\ &Subject\ to \quad X^l \le X \le X^u \end{aligned} \quad (8)$$

In this work, parameter x ranged from 0 to 0.5 for the first and the third example and ranged from 0 to 0.3 for the second test example.

3. Introducing Echolocation search algorithm (ESA)

Due to industrial and scientific developments many complex optimization problems are needed to be solved. Having discrete variables, high dimensional and none differential are some characteristics of most of these problems. Then traditional optimization methods can't help us to solve them. To overcome this difficulty, in the 1950s and the 1960s the idea of utilizing an evolutionary technique as an optimization tool for engineering problems was developed. Since then many heuristic search algorithms were developed. Some of the novel heuristic algorithms are harmony search proposed by Geem *et al*. (2001), gravitational search algorithm proposed by Rashedi *et al*. (2009), charged system search presented by Kaveh and Talatahari (2010), water cycle algorithm proposed by Eskandar *et al*. (2012), Dolphin Echolocation proposed by Kaveh and Farhoudi (2013).

In this paper, inspired by animals such as bat, dolphin, oilbird, shrew etc. that use echolocation for finding food, a new and efficient method for finding the optimum points is introduced. In ESA, first a point is randomly selected in the searching space assigned as the primary location of the echolocating animal (EA). The Echolocating Animal's Location (*EAL*) is a d dimensional vector being the corresponding number of variables. The objective function and its degree of constraints satisfaction are evaluated for EA in its current Location. Then, the EA sends nw waves in various directions randomly. Each wave, in its own direction, randomly hits a candidate as an object. The fitness of that object is calculated and the wave then returns to the EA. The EA now, according to the information it has about the validity of each nw point around its location and by the use of relations which will be introduced in the following sections, will compute nw new points, that is nw new candidates. Then it sends waves to these new points to estimate their bigness (calculating their objective functions). Furthermore, according to 3 top points have been discovered so far, the EA calculates a direction for movement and proceeds in that direction. This continues until reaching convergence to the optimum point or it terminates.

Regarding the above explanations, in each iteration nw+1 time analysis takes place. nw time relates to points to which the wave is sent, and 1 stands for another analysis associated to the *EAL*. In this method, for obtaining new points, all points share the same chance for training the EA. In other words, the EA enjoys from information, even from the weakest points. Through observation and comparison of the weak and strong points, the EA will identify points which are likely to be stronger. However, 3 top points among nw+1 points play a considerable role in the education and movement of the EA. In fact, the EA analyzes its direction only by the prior 3 top points. Additionally, one of the coordinates of nw new points will certainly be computed by the primary 3 top points.

The general ESA flowchart is as given in Fig. 1. In the next section, all stages related to the flowchart will be described in details.

3.1 Select the primary location of the echolocating animal (EA)

To begin with, first the EAL is randomly selected

$$EAL = \{x_1, x_2, \dots, x_d\} \quad (9)$$

Where x_i is the value of the i^{th} variable of *EAL* vector. Also, d denotes search space dimension or the number of the problem variables. Then, the value of the objective function relevant to *EAL* is computed

$$POEL = objfunction(EAL) \quad (10)$$

In the above relation, *objfunction ()* is the objective function to be optimized. *POEL* is the value of the objective function related to the current *EAL*. According to the Eq. (9), *EAL* is the vector of the echolocating animal location.

3.2 Send stochastic waves and locate a point along each wave

The EA randomly sends *nw* waves and each wave selects a point in its own direction stochastically. Therefore, *nw* points are randomly created. The result is the creation of *POINT* matrix which is a *nw*× *d* matrix as follows

$$POINT = \begin{bmatrix} x_{1,1} & \dots & x_{1,d} \\ \vdots & x_{i,j} & \vdots \\ x_{nw,1} & \dots & x_{nw,d} \end{bmatrix} \quad (11)$$

where, x_{ij} stands for j^{th} variable related to i^{th} point.

3.3 Calculate objective function value of points

At this stage of procedure, there are *nw*+1 coordinates that consist of the current *EAL* and *nw* points around the EA in the space. The objective function value at the *nw* specified points should be calculated and for training and making decision, it should be sent back to the EA. To do this, the value of the objective function in the above points is calculated

$$\{f_1, \dots, f_{nw}\} = objfunction(POINT) \quad (12)$$

In the above relation, f_i is the value of the objective function in the i^{th} point. Now, there are *nw*+1 points plus their objective functions.

3.4 Determine top three points of all iterations so far

After having computed the objective values, coordinates of the top three points' so far will be saved in the EA's memory in the form of a matrix named *BESTP*

$$BESTP = \begin{bmatrix} bx_{1,1} & \dots & bx_{1,d} \\ bx_{2,1} & \dots & bx_{2,d} \\ bx_{3,d} & \dots & bx_{3,d} \end{bmatrix} \quad (13)$$

$$BESTV = \{bestv_1, bestv_2, bestv_3\} \quad (14)$$

In Eqs. (13)-(14), $bestv_1$ is the value of the objective function for the optimum point so far and $bx_{1,1}$ through $bx_{1,d}$ are the values of the coordinates related to this point. $bestv_2$ and $bestv_3$ are the values of the objective function of the second and third top points in all prior iterations, respectively.

3.5 Termination criteria?

After the determination of the top three points in all prior iterations, termination criteria will be examined. Like other methods, in the ESA two types of termination condition, dependent on the answer and independent of the answer, can be adapted.

3.6 Satisfies criterion of specifying variables domains?

If the modification of the best point in the certain prior iterations is less than a certain value that determined by user, search space is limited and new points are generated in new search space stochastically. Otherwise ESA behaves in another way. In following all of these described in details.

3.7 Specify lower and upper bounds for each design variable

If the criterion of specifying variables domain satisfied, the EA considers the best point it has found so far and extenuate the scope around the best point. In other words, it will slightly narrow down the search space. The restriction amount of the scope will be given to the EA through a *rbf* coefficient whose positive value is smaller than 1. In this stage, the EA computes a new domain considering the following relation

$$ndomain_i = rbf.pdomain_i \quad i = 1{:}\,d \quad (15)$$

In the above relation, *d* is number of variables, $ndomain_i$ length of new domain related to the i^{th} variable, $pdomain_i$ is the length of the previous domain of i^{th} variable and the *rbf* is coefficient of the reduction range. Upper and lower bounds for each variable calculated according to below relations

$$\begin{aligned} x_i^{u^*} &= \min(bx_{1,i} + 0.5 * ndomain_i, x_i^u) \\ x_i^{l^*} &= \max(x_i^{u^*} - ndomain_i, x_i^l) \quad i = 1{:}\,d \end{aligned} \quad (16)$$

In these relations $x_i^u$and x_i^l are upper and lower bounds for the i^{th} design variable. $x_i^{u^*}$ and $x_i^{l^*}$ are new upper and lower bounds for i^{th} design variable respectively. bx_{1i} is the value of i^{th} design variable in best point.

3.8 Adapt Stochastically New Points Along the New Waves Generated

After determination of the new search space boundaries, EA emitted *nw* waves stochastically and in this way generated *nw* stochastically points in new search space.

3.9 Produce new points based on the proposed method

If the criterion of specifying variables domain was not satisfied, in this stage, according to the received data from points around, the EA prepares itself and computes the new coordinates to send waves. For achieving the coordinates of *nw* new points, the EA enjoys all information obtained from the previous iteration's points. To do this, the EA chooses three stochastic points and then arrange them according to the object of the problem. Now there are three points P_1, P_2 and P_3 ranking 1, 2 and 3, respectively. The EA at first estimates the disparity of the coordinate of points 1, 2 and 2, 3 as follow

$$\begin{aligned} DELTA1 &= P_1 - P_2 = \{x_{1,1} - x_{2,1}, \dots, x_{1,d} - x_{2,d}\} \\ DELTA2 &= P_2 - P_3 = \{x_{2,1} - x_{3,1}, \dots, x_{2,d} - x_{3,d}\} \end{aligned} \quad (17)$$

Now, the movement direction from P_2 to P_1 and P_3 to P_2 in each dimension is achieved by the use of the *sign()* function, which reverses its parameter sign

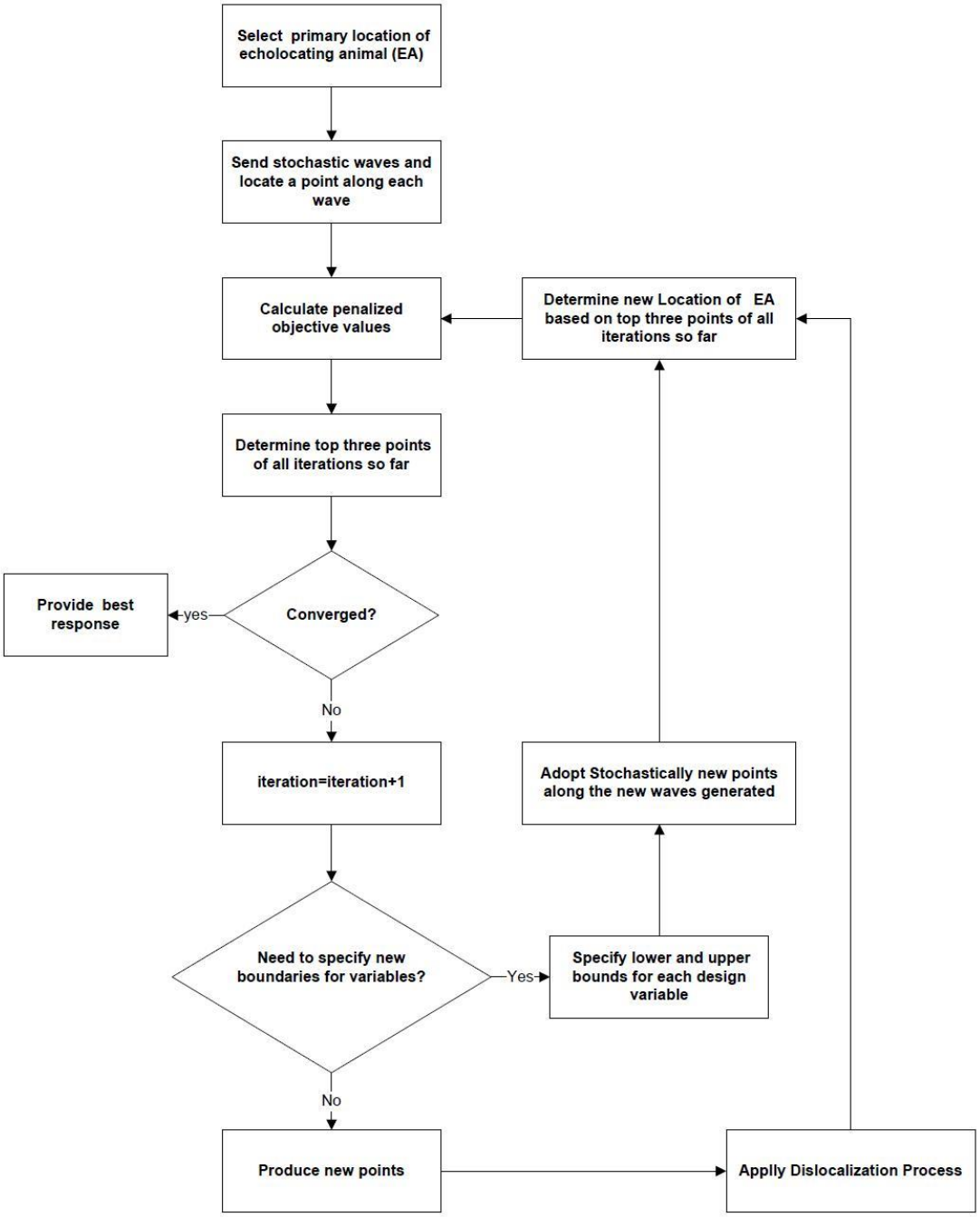

Fig. 1 Flowchart of Echolocation Search Algorithm (ESA)

$$DIRECT1 = sign(DELTA1) = \{s_{1,1}, \dots., s_{1,d}\}$$
$$DIRECT2 = sign(DELTA2) = \{s_{2,1}, \dots., s_{2,d}\} \quad (18)$$

For instance, $s_{1,2}$ is the value of the *sign* ($x_{1,2}$-$x_{2,2}$). So if $x_{1,2}$-$x_{2,2}$ is positive, $s_{1,2}$will be equal to 1 and if it is negative $s_{1,2}$ will be -1. Finally, if it is equal to zero then $s_{1,2}$ will become 0. Now, for the calculation of the new point, we multiply peer by peer of both vectors by each other. The resulted vector will have *NDIR*.

$$NDIR = DIRECT1 \otimes DIRECT2 = \{dr_1, \dots., dr_d\} \quad (19)$$

In this relation, the sign $\otimes$ implies the multiplication of peer by peer of the two vectors

$$dr_i = s_{1,i} \times s_{2,i} \qquad i = 1{:}\,d \quad (20)$$

dr_i can have one of three values, 1,0,-1. If dr_i=1 it means that movement direction in the i^{th} dimension from P_3 toward P_2 is similar to the movement direction in the same dimension from P_2 to P_1. In other words, both are either ascending or descending. Therefore, movement in this direction may improve the answer. It can be shown in mathematical form as follows

$$dr_i = 1 \Rightarrow \begin{cases} x_{3,i} < x_{2,i} < x_{1,i} \Rightarrow nx_{j,i} > x_{1,i} \\ x_{3,i} > x_{2,i} > x_{1,i} \Rightarrow nx_{j,i} < x_{1,i} \end{cases} \quad (21)$$

In the relation, $nx_{j,i}$ stands for the i^{th} variable from the j^{th} new point. As a result, the EA computes the coordinates of the new point through the following formula

$$nx_{j,i} = x_{1,i} + rand \times (x_{1,i} - x_{2,i}) \quad (22)$$

rand is a random value in the range [0,1] and *i* indicates the number of variables. If dr_i=0, it means that either $x_{1,i}$=$x_{2,i}$ or $x_{2,i}$=$x_{3,I}$ or both are applicable. If dr_i possesses a zero value due to the relation of $x_{1,i}$=$x_{2,i}$ then most likely this value will be suitable for the i^{th} dimension. If $x_{2,i}$=$x_{3,I}$ then the movement from $x_{2,i}$ to $x_{1,i}$will be appropriate. In each case, Eq. (22) is useful. The following formula certifies the above statements

$$dr_i = 0 \Rightarrow \begin{cases} x_{3,i} = x_{2,i} > x_{1,i} \Rightarrow nx_{j,i} < x_{1,i} \\ x_{3,i} = x_{2,i} < x_{1,i} \Rightarrow nx_{j,i} > x_{1,i} \\ x_{3,i} = x_{2,i} = x_{1,i} \Rightarrow nx_{j,i} = x_{1,i} \\ x_{3,i} > x_{2,i} = x_{1,i} \Rightarrow nx_{j,i} = x_{1,i} \\ x_{3,i} < x_{2,i} = x_{1,i} \Rightarrow nx_{j,i} = x_{1,i} \end{cases} \quad (23)$$

But if dr_i<0, then movement from P_3 to P_2 and from P_2 to P_1 in the i^{th} dimension is in opposite direction. So, it is impossible to decide on the movement direction. In this condition, the EA with 50 % probability will choose $x_{1,I}$ or $x_{2,I}$ for $nx_{j,i}$. It can be mathematically represented as shown below

$$dr_i = -1 \Rightarrow \begin{cases} x_{1,i} < x_{2,i} > x_{3,i} \\ \\ x_{1,i} > x_{2,i} < x_{3,i} \end{cases} \Rightarrow \begin{matrix} nx_{j,i} = x_{1,i} \\ or \\ nx_{j,i} = x_{2,i} \end{matrix} \quad (24)$$

For example suppose each design has 8 variables and the search space domain of each design variable is [1, 50]. If the three points that stochastically selected to generate a new point were as shown in Fig. 2, so that P_1, P_2 and P_3 have best fitness, mid fitness and least fitness among their self, respectively. In this case according to relations that described above, the new point which shown in Fig. 2, can be a probable point that generated. The EA obtains the coordination of one point out of *nw* points through the use of three top points.

3.10 Apply dislocalization technique (DT)

During optimization process by the ESA, it is possible that all points in one or more dimensions become convergent in special values. If these values are not appropriate, this directs the answer toward improper convergence. To avoid this, when the coefficient of variation of each variable is less than that of user-defined values (cv_{min}), the EA randomly changes the value of these variables in a certain percent of points. Selection of points and the new value of the variables will be done stochastically. The new value can be chosen in the primary range defined at the beginning.

Points	X1	X2	X3	X4	X5	X6	X7	X8
P1	5.41	39.67	50	1	19.14	28.65	23.12	23.89
P2	7.96	21.23	38.76	13.27	12.45	45.12	23.12	13.67
P3	12.23	8.93	9.12	23.19	12.45	45.12	9.56	21.87
	⇩	⇩	⇩	⇩	⇩	⇩	⇩	⇩
New point	3.11	43.97	50	1	22.64	17.83	23.12	13.67

Fig. 2 New generated points using previous information

3.11 Determining new location of echolocating animal (EAL)

To determine the direction of movement, EA enjoys the three top points. To do this, first the fitness value of these three points will be obtained. The fitness value should be a positive one. The fitness value of the point is calculated as shown below. If the aim is to compute the maximum value of the function, the fitness function is as follows

$$fit_i = bestv_i + c_{max} + c_{min} \quad i = 1{:}3 \quad (25)$$

where $bestv_i$ and fit_i are the value of objective function and fitness value of the i^{th} top point respectively

$$\begin{matrix} c_{max} = |\max(bestv_i)| \\ c_{min} = |\min(bestv_i)| \end{matrix} \quad i = 1{:}3 \quad (26)$$

If the aim is to compute the minimum value of function, the fitness function will be achieved by the following relation

$$fit_i = c_{max} + c_{min} - bestv_i \quad (27)$$

The EA estimates the coordinates of the end point of the movement vector form the following relation

$$epoint = \sum_{i=1}^{3} \frac{fit_i . BP_i}{tfit} \quad (28)$$

Where BP_i is coordinate's vector of i^{th} top point or in other words it is the i^{th} row of *BESTP* described in Eq. (13), and *tfit* is calculated by the following relation

$$tfit = \sum_{i=1}^{3} fit_i \quad (29)$$

The new place of EA is achieved via the relation given as

$$NEAL = EAL + rand \times (epoint - EAL) \quad (30)$$

where *EAL* is the current location of the EA, *NEAL* is the new location of the EA and *rand* is a random value in the range [0,1]. This procedure continues until convergence criteria are met.

4. Test examples

In this section, in order to show the capabilities of the proposed algorithm for identifying structural damage, three illustrative test examples are considered. The first example is a 31-bar planar truss, the second one is 10-bar planar truss and the last example is a 47-bar planar truss. The first and the second examples do not consider the measurement noise, however the third example is studied in two circumstances of noise-free and noisy measurement data.

4.1 Thirty one bar-planar truss

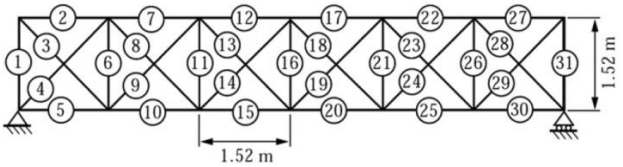

Fig. 3 The 31-element planar truss

The 31-bar planar truss shown in Fig. 3 is selected from (Mesina *et al*. 1998). In this example the first ten natural frequencies are utilized for damage identification. The material density and elasticity modulus are 2770 kg/m^3 and 70 GPa, respectively. Based on (Mesina *et al*. 1998), the stiffness reduction caused by the damage is smaller than 50% for this example.

Number of waves is set to 19. Thus, 20 evaluations including location of the echolocating animal are carried out in each iteration. The maximum number of iterations, the minimum coefficient of variation ($cv_{\min}$) and the reduced boundary factor (*rbf*) are set to 1000, 0.01 and 0.9, respectively. The convergence of ESA is meant to occur when the *ECBI* differs a fraction of $1*10^{-5}$ of the target value, or the maximum number of iterations is reached.

Based on (Mesina *et al*. 1998), two Scenarios are set as follows:

Scenario1: 25% damage in element 11 and 15% damage in element 25.

Scenario2: 30% damage in element 1 and 20% damage in element 2.

According to (Nobahari and Seyedpoor 2011), ten independent runs are carried out for each Scenario using the proposed technique. The results of damage identifications for the two Scenarios are given in Tables 1 and 2. The average of damage ratios obtained in (Nobahari and Seyedpoor 2011, Shirazi *et al*. 2014) and their corresponding number of analyses required were shown in these tables for comparison.

According to the results shown in Tables 1-2, the robustness of ESA in identifying the location and severity of structural damage is comparable with GA (Nobahari and Seyedpoor 2011) and MPSO (Shirazi *et al*. 2014) . It is to be noted that the damage ratios were considered as discrete variables in (Nobahari and Seyedpoor 2011) which obviously reduces the search space significantly and one would have expected less number of analyses accordingly.

4.2 Ten bar planar truss

The 10-bar planar truss shown in Fig. 6 is considered as the second example. The stiffness reduction caused by the damage is smaller than 30%. The material density, elasticity modulus and cross sectional area are set to 2770 kg/m^3, 69.8 GPa and 0.0025 m^2, respectively. The optimization parameters are the same as the first example. According to (Kaveh and Zolghadr 2015) the first 8 natural frequencies are utilized for damage detection.

This example employs two Scenarios:

Scenario 1: 5% damage in element 1(5% damage in element 3 will result in the same set of natural frequencies)

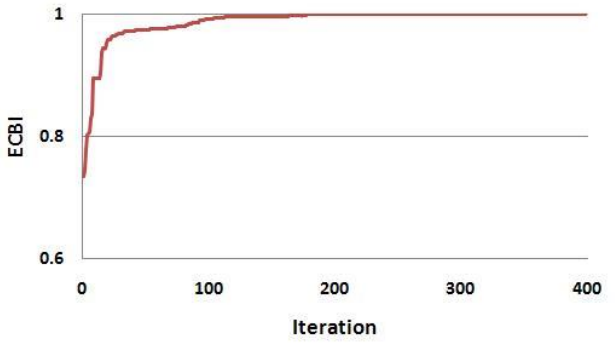

Fig. 4 Convergence history of the 31-bar planar truss for Scenario 1 obtained by ESA

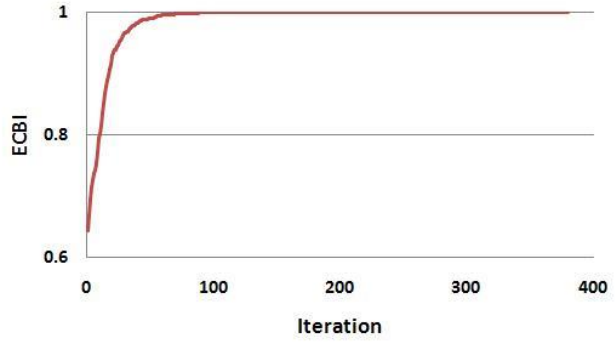

Fig. 5 Convergence history of the 31-bar planar truss for Scenario 2 obtained by ESA

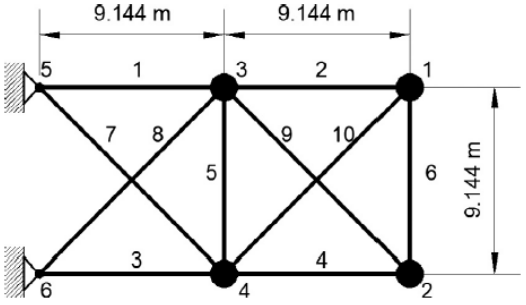

Fig. 6 10-bar planar truss

Scenario 2: 10% damage in element 2 and 5% damage in element 4.(5% damage in element 2 and 10% damage in element 4 will result in the same set of natural frequencies)

Due to stochastic nature of optimization algorithm, ten independent runs are made for each damage case. The results of damage identification for this example are given in Tables 3-4.

As it is shown in Tables 3 and 4 and emphasized by Kaveh and Zolghadr (2015), the proposed algorithm could clarify the fact that two different damage Scenarios may cause identical frequency variations while the output for the function value is equal to one in both.

4.3 Forty seven-bar planar truss

The final example investigated here is a 47-bar planar

power line tower, shown in Fig. 9. The material density, elasticity modulus and cross sectional area for the problem are 0.3 lb/in^3, 30000 ksi and 3.87 in^2, respectively. In this example the first 10 natural frequencies are utilized for detection of damage. In order to investigate the effect of measurement noise on the performance of the proposed algorithm, the measurement noise is considered by riddling the natural frequencies using a standard error of $\pm$0.15%. The optimization parameters are kept the same as the first example. Two Scenarios are set as follows:

Scenario 1: 30% damage in element 10.

Scenario 2: 30% damage in element 10 and 30% damage in element 30.

Due to stochastic nature of optimization algorithm, ten independent runs are made for each damage case. The results of damage identification without considering measurement noise are given in Tables 5-6.

In this example, to investigate the ability of ESA in detecting the severity and extents of damages using the proposed algorithm, the GA was run and the obtained results were compared as shown in Tables 5-10.

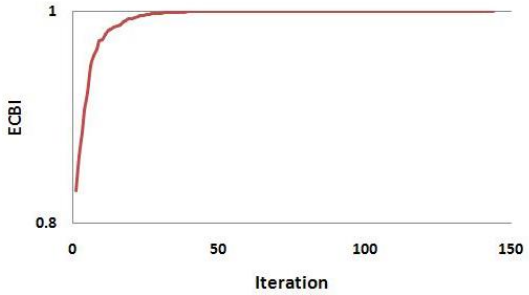

Fig. 7 Convergence history for the 10-bar planar truss for Scenario 1 obtained by ESA

Table 1 The damage percentage of the 31-bar truss for Scenario 1

Run no	1	…	10	11	12	…	23	24	25	26	…	30	31	No. analyses carried
1	0	0	0	25	0	0	0	0	15	0	0	0	0	6380
2	0	0	0	25	0	0	0	0	15	0	0	0	0	6720
3	0	0	0	25	0	0	0	0	15	0	0	0	0	5420
4	0	0	0	25	0	0	0	0	15	0	0	0	0	6720
5	0	0	0	25	0	0	0	0	15	0	0	0	0	5920
6	0	0	0	25	0	0	0	0	15	0	0	0	0	4480
7	0	0	0	25	0	0	0	0	15	0	0	0	0	5500
8	0	0	0	25	0	0	0	0	15	0	0	0	0	9760
9	0	0	0	25	0	0	0	0	15	0	0	0	0	5460
10	0	0	0	25	0	0	0	0	15	0	0	0	0	7040
Average damage %	0	0	0	**25**	0	0	0	0	**15**	0	0	0	0	**6340**
MPSO-based damage %	0	0	0	24.95	0	0	0	0	14.96	0	0	0	0	35700
GA-based damage %	0	0	0	26.5	0	0	0	0	18	0	0	0	0	8910
Actual damage %	0	0	0	25	0	0	0	0	15	0	0	0	0	

Table 2 The damage percentage of the 31-bar truss for Scenario 2

Run no	1	2	3	…	13	14	…	24	25	26	27	…	31	No. analyses carried
1	30	20	0	0	0	0	0	0	0	0	0	0	0	7820
2	30	20	0	0	0	0	0	0	0	0	0	0	0	2680
3	30	20	0	0	0	0	0	0	0	0	0	0	0	3720
4	30	20	0	0	0	0	0	0	0	0	0	0	0	6700
5	30	20	0	0	0	0	0	0	0	0	0	0	0	3220
6	30	20	0	0	0	0	0	0	0	0	0	0	0	4820
7	30	20	0	0	0	0	0	0	0	0	0	0	0	10800
8	30	20	0	0	0	0	0	0	0	0	0	0	0	2200
9	30	20	0	0	0	0	0	0	0	0	0	0	0	4640
10	30	20	0	0	0	0	0	0	0	0	0	0	0	2900
Average damage %	**30**	**20**	0	0	0	0	0	0	0	0	0	0	0	**4950**
MPSO-based damage %	30	20	0	0	0	0	0	0	0	0	0	0	0	33900
GA-based damage %	30	20	0	0	0	0	0	0	0	0	0	0	0	6391
Actual damage %	30	20	0	0	0	0	0	0	0	0	0	0	0	

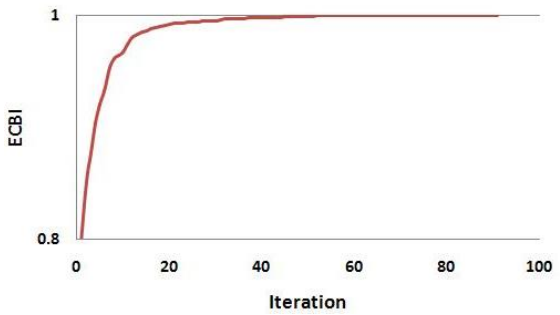

Fig. 8 Convergence history for the 10-bar planar truss for Scenario 2 obtained by ESA

Table 3 The damage percentage of the 10-bar truss for Scenario 1

Run no	1	2	3	…	10	ECBI	No. analyses carried
1	5	0	0	0	0	1	660
2	0	0	5	0	0	1	720
3	5	0	0	0	0	1	1000
4	5	0	0	0	0	1	720
5	5	0	0	0	0	1	500
6	0	0	5	0	0	1	1020
7	5	0	0	0	0	1	720
8	5	0	0	0	0	1	720
9	0	0	5	0	0	1	720
10	5	0	0	0	0	1	720
Average						1	**750**
Actual damage %	5	0	0	0	0		
Actual damage %	0	0	5	0	0		

According to the results given in Tables 5 and 6, ESA could find the location and severity of damaged members with an acceptable accuracy.

In this example for both Scenarios, ESA could detect damaged members for all runs. Also in both Scenarios, for 70% of runs, the damage severity evaluated by ESA is exact and for 30% of runs, the estimated damage severity is very close to actual value.

For example, in Scenario 1, the mean value of evaluated damage severity for damaged member (element 10) is 29.6% which has a little divergence with real value (30%). In Scenario 2, the mean value of evaluated damage severity for damaged members (elements 10 and 30) are 27.9% and 29.8% which are very close to real value (30%). Thus in general, one would observe that the discrepancy is very small and negligible. Also it is worth to note that although the damage variables were considered discrete in GA, the number of analyses carried out in GA was greater than that of ESA.

Although achieving the target value of ECBI (1) by considering measurement noise is impossible but according to Figs. 10-11, ESA could achieve 0.995 after approximately 250 iterations.

Table 4 The damage percentage of the 10-bar truss for Scenario 2

Run no	1	2	3	4	..	10	ECBI	No. analyses carried
1	0	10	0	5	0	0	1	1080
2	0	10	0	5	0	0	1	1020
3	0	5	0	10	0	0	1	1020
4	0	5	0	10	0	0	1	1040
5	0	10	0	5	0	0	1	1020
6	0	5	0	10	0	0	1	1020
7	0	5	0	10	0	0	1	1260
8	0	10	0	5	0	0	1	1020
9	0	5	0	10	0	0	1	1020
10	0	10	0	5	0	0	1	720
Average							1	1022
Actual damage %	0	10	0	5	0	0		
Actual damage %	0	5	0	10	0	0		

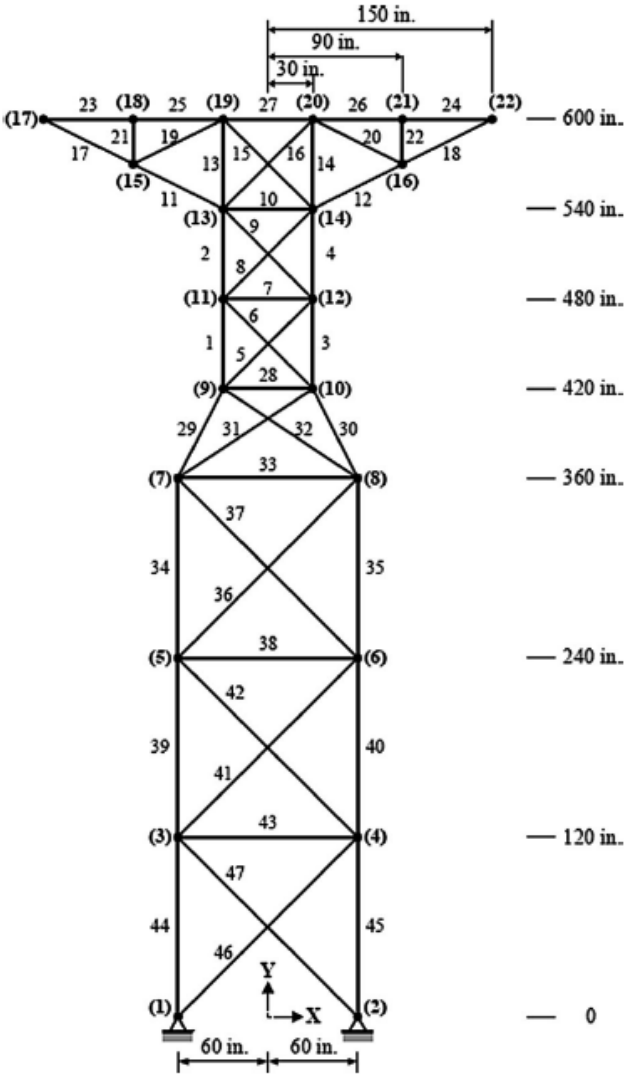

Fig. 9 The 47-bar planar power line tower

Table 5 The damage percentage of the 47-bar planar power line tower for Scenario 1 with free noise data

Run no	1	…	7	8	9	10	11	…	21	22	23	…	47	No. analyses carried
1	0	0	1	0	0	29	0	0	0	0	0	0	0	6300
2	0	0	0	0	0	30	0	0	0	0	0	0	0	7620
3	0	0	0	0	0	30	0	0	1	0	0	0	0	4580
4	0	0	0	0	0	29	0	0	0	0	0	0	0	5680
5	0	0	0	0	0	30	0	0	0	2	0	0	0	5820
6	0	0	0	0	0	30	0	0	0	0	0	0	0	4780
7	0	0	0	0	0	30	0	0	0	0	0	0	0	5760
8	0	0	0	0	0	29	0	0	0	0	0	0	0	7080
9	0	0	0	0	0	30	0	0	0	0	0	0	0	3860
10	0	0	0	0	0	30	0	0	0	0	0	0	0	5960
Average damage %	0	0	0.1	0	0	29.6	0	0	0.1	0.2	0	0	0	5744
GA-based damage %	0	0	0	0	2	29.5	1.5	0	0	0	0	0	0	10060
Actual damage %	0	0	0	0	0	30	0	0	0	0	0	0	0	

Table 6 The damage percentage of the 47-bar planar power line tower for Scenario 2 with free noise data

Run no	1	…	8	9	10	11	…	22	…	30	31	32	33	...	47	No. analyses carried
1	0	0	0	0	30	0	0	0	0	30	0	0	0	0	0	5740
2	0	0	0	0	30	0	0	0	0	30	0	0	0	0	0	6720
3	0	0	0	0	30	0	0	0	0	30	0	0	0	0	0	5580
4	0	0	0	0	30	0	0	0	0	30	0	0	0	0	0	6660
5	0	0	1	0	30	0	0	0	0	30	0	0	0	0	0	10180
6	0	0	0	0	30	0	0	0	0	30	0	0	0	0	0	10300
7	0	0	0	0	28	1	0	0	0	30	0	0	0	0	0	20000
8	1	0	3	0	20	2	0	0	0	29	0	0	2	0	0	20000
9	0	0	1	0	30	0	0	0	0	30	0	0	0	0	0	12420
10	1	0	3	0	21	2	0	2	0	29	0	0	2	0	0	20000
Average damage %	0.2	0	0.8	0	27.9	0.5	0	0.2	0	29.8	0	0	0.4	0	0	11760
GA-based damage %	0	0	0	0	25.5	0.5	0	0	0	35	0	1	0	0	0	18460
Actual damage %	0	0	0	0	30	0	0	0	0	30	0	0	0	0	0	

Table 7 The damage percentage of the 47-bar planar power line tower for Scenario 1 with noisy data

Run no	1	…	7	8	9	10	11	…	18	…	20	21	…	46	47	No. analyses carried
1	2	0	9	0	0	24	0	0	0	0	0	0	0	1	0	20000
2	0	0	0	0	0	20	0	0	1	0	0	0	0	1	1	20000
3	0	0	0	6	0	45	4	0	0	0	0	0	0	0	0	20000
4	0	0	0	3	0	17	0	0	0	0	10	0	0	0	0	20000
5	0	0	0	0	0	34	0	0	2	0	2	2	0	0	0	20000
6	0	0	3	0	7	17	0	0	5	0	0	5	0	0	0	20000
7	1	0	2	0	0	15	2	0	0	0	1	0	0	5	0	20000
8	0	0	0	0	0	42	0	0	0	0	0	0	0	0	0	20000
9	0	0	0	9	0	12	0	0	0	0	0	0	0	0	0	20000
10	0	0	0	0	2	11	2	0	0	0	0	10	0	0	0	20000
Average damage %	0.3	0	1.4	1.8	0.9	**26.7**	0.8	0	0.8	0	1.3	1.7	0	0.7	0.1	20000
Actual damage %	0	0	0	0	0	30	0	0	0	0	0	0	0	0	0	

Table 8 The damage percentage of the 47-bar planar power line tower for Scenario 2 with noisy data

Run no	1	…	8	9	10	11	…	22	…	28	29	30	…	33	…	43	…	47	No. analyses carried
1	0	0	0	3	15	0	0	0	0	0	0	29	0	0	0	1	0	0	20000
2	0	0	10	0	12	0	0	0	0	0	0	27	0	0	0	0	0	0	20000
3	0	0	12	7	19	0	0	0	0	2	0	29	0	0	0	8	0	0	20000
4	0	0	0	0	28	0	0	0	0	0	0	30	0	0	0	0	0	0	20000
5	0	0	7	1	10	4	0	10	0	0	0	28	0	4	0	0	0	0	20000
6	0	0	0	0	11	0	0	9	0	5	0	29	0	0	0	1	0	0	20000
7	0	0	0	0	13	2	0	0	0	0	3	21	0	0	0	0	0	0	20000
8	0	0	8	0	10	1	0	2	0	8	0	27	0	2	0	0	0	0	20000
9	0	0	0	0	32	0	0	0	0	12	0	30	0	0	0	1	0	0	20000
10	0	0	0	3	16	1	0	1	0	0	0	21	0	1	0	0	0	0	20000
Average damage %	0	0	3.7	1.4	**16.6**	0.8	0	2.2	0	2.7	0.3	**27.1**	0	0.7	0	1.1	0	0	20000
Actual damage %	0	0	0	0	30	0	0	0	0	0	0	30	0	0	0	0	0	0	

Table 9 The results for the damage detection of the 47-bar planar truss, Scenario 1 with noisy data, using GA

Run no	1	…	6	7	8	9	10	11	…	15	16	….	47	No. analyses carried
1	0	0	0	10	5	0	45	15	0	0	0	0	0	20000
2	**0**	**0**	**10**	**20**	**25**	**35**	**0**	**0**	**0**	**0**	**0**	**0**	**0**	**20000**
3	0	0	0	0	25	35	15	0	0	0	0	0	0	20000
4	**0**	**0**	**0**	**0**	**15**	**45**	**0**	**0**	**0**	**10**	**0**	**0**	**0**	**20000**
5	0	0	0	0	10	10	25	0	0	10	15	0	0	20000
6	**0**	**0**	**0**	**0**	**15**	**25**	**0**	**0**	**0**	**15**	**0**	**0**	**0**	**20000**
7	0	0	0	0	10	0	45	0	0	0	0	0	0	20000
8	0	0	0	0	15	5	50	0	0	0	10	0	0	20000
9	0	0	0	0	5	0	25	0	0	15	10	0	0	20000
10	**0**	**0**	**0**	**0**	**0**	**45**	**0**	**0**	**0**	**10**	**0**	**0**	**0**	**20000**
Average damage %	0	0	1	3	12.5	19.5	20.5	1.5	0	6	3.5	0	0	20000
Actual damage %	0	0	0	0	0	0	30	0	0	0	0	0	0	

Table 10 The results for the damage detection of the 47-bar planar truss, Scenario 2 with noisy data, using GA

Run no	1	2	3	…	6	7	8	9	10	11	…	30	31	32	…	35	…	47	No. analyses carried
1	0	0	0	0	0	0	0	25	15	0	0	40	0	0	0	20	0	0	20000
2	0	0	0	0	0	0	10	0	25	0	0	50	0	0	0	0	0	0	20000
3	0	0	20	0	10	0	0	0	45	0	0	25	0	0	0	0	0	0	20000
4	0	0	20	0	25	0	0	0	35	0	0	45	0	0	0	0	0	0	20000
5	**0**	**0**	**10**	**0**	**0**	**0**	**0**	**45**	**0**	**0**	**0**	**40**	**0**	**0**	**0**	**0**	**0**	**0**	20000
6	0	0	0	0	20	0	0	10	25	0	0	35	0	10	0	0	0	0	20000
7	0	0	0	0	0	0	20	0	15	0	0	35	0	0	0	0	0	0	20000
8	0	0	0	0	15	0	0	0	40	0	0	50	0	0	0	0	0	0	20000
9	0	0	0	0	10	0	0	0	45	0	0	50	0	0	0	10	0	0	20000
10	0	0	0	0	0	0	5	0	35	0	0	45	0	0	0	0	0	0	20000
Average damage %	0	0	5	0	8	0	3.5	8	27	0	0	46.5	0	1	0	3	0	0	20000
Actual damage %	0	0	0	0	0	0	0	0	30	0	0	30	0	0	0	0	0	0	

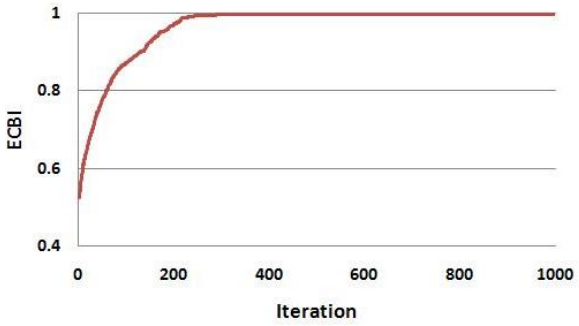

Fig. 10 Convergence history of the 47-bar planar truss for Scenario 1 obtained by ESA

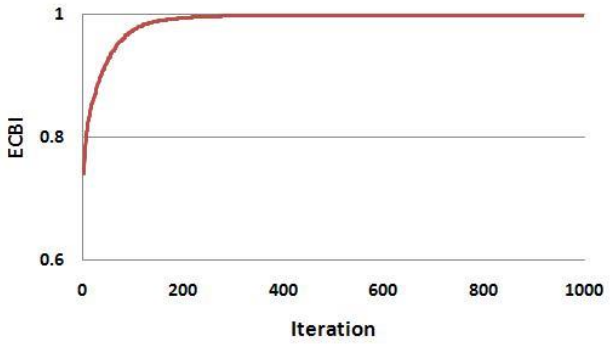

Fig. 11 Convergence history of the 47-bar planar truss for Scenario 2 obtained by ESA

Existence of measurement noise converts the damage detection problem to a complicated one. In these cases, a precise damage severity assessment is very difficult if not impossible and damage localization is more important than damage severity assessment. If damage extents are needed to be evaluated accurately, other measurement data such as mode shapes may also be needed. As presented in Tables 7 and 8, ESA could detect damaged members in all runs for both the damage Scenarios. Also estimated damage severities by ESA is adjacent to reality and may be regarded as acceptable. However, according to Table 9, for the first Scenario, in 40% of runs, GA could not detect the damage location (bolded in the table). Also, as depicted in Table 10, for the second Scenario, GA was ineffective to detect the damaged members in 10% of runs (bolded in table).

5. Conclusions

In this paper a vibration-based structural damage identification was conducted as an inverse optimization problem. To solve such problems, there are several search algorithms such as GA, PSO etc. In this paper by mimicking from strategies used by echolocation animals such as bats, dolphins, oilbirds, shrews etc. searching for food and navigation, a novel heuristic search algorithm (ESA) was proposed. Although searching process in the proposed algorithm, similar to other heuristic search algorithms, is based on stochastic laws, its governing rules are less chaotic compared to other search algorithms. This feature helped the authors to solve the three numerical optimization problems with lower computational efforts.

The first example was a 31 elements planar truss, for which two damage Scenarios were considered. The results of the first Scenario showed that ESA could meet the exact response by approximately 18% of computational cost using MPSO. Besides, although in GA, the damage variables were considered as discrete, as a result of which one would expect the size of search space to be reduced compared to continuous type of variables, the required computational cost by ESA was found 71% lower than GA and also more accurate. In the second damage Scenario, superiority of ESA results was clearly evident when compared to those based on GA or MPSO. ESA could obtain the exact solution by 4950 analyses, nearly seven times that of MPSO and 1.5 times that of GA.

The second example was a 10-bar planar truss. In this example, ESA confronted a challenging dilemma. Two different frequency diversities were studied, each of which had two different responses. Thus, two different damage Scenarios causing identical natural frequency changes were correctly detected by ESA.

As the last example, a 47-bar planar truss with two different damage Scenarios was studied. In this example to investigate the robustness of ESA, the measurement noise was considered. Existence of measurement noise obscures the structural damage detection problems. Exact damage severity assessment by just utilizing the noisy natural frequencies is an impossible task. In that respect, for both damage Scenarios in this example, ESA could detect damaged elements properly and the damage severity approximated by ESA had a satisfactory accuracy.

References

Baghmisheh, M.V., Peimani, M., Sadeghi, M.H., Ettefagh, M.M. and Tabrizi, A.F. (2012). "A hybrid particle swarm-Nelder-Mead optimization method for crack detection in cantilever beams", *Appl. Soft Comput.*, **12**(8), 2217-2226.

Begambre, O. and Laier, J.E. (2009), "A hybrid particle swarm optimization-simplex algorithm (PSOS) for structural damage identification", *Adv. Eng. Softw.*, **40**(9), 883-891.

Eskandar, H., Sadollah, A., Bahreininejad, A. and Hamdi, M. (2012), "Water cycle algorithm-a novel metaheuristic optimization method for solving constrained engineering optimization problems", *Comput. Struct.*, **110**, 151-166.

Geem, Z.W., Kim, J.H. and Loganathan, G.V. (2001), "A new heuristic optimization algorithm: harmony search", *Simulation*, **76**(2), 60-68.

He, R.S. and Hwang, S.F. (2006), "Damage detection by an adaptive real-parameter simulated annealing genetic algorithm", *Comput. Struct.*, **84**(31), 2231-2243.

Kang, F. and Li, J. (2015), "Artificial bee colony algorithm optimized support vector regression for system reliability analysis of slopes", *J. Comput. Civ. Eng.*, **30**(3), 04015040.

Kang, F., Li, J.J. and Xu, Q. (2012), "Damage detection based on improved particle swarm optimization using vibration data", *Appl. Soft Comput.*, **12**(8), 2329-2335.

Kang, F., Xu, Q. and Li, J. (2016), "Slope reliability analysis using surrogate models via new support vector machines with swarm intelligence", *Appl. Math. Model.*, **40**(11), 6105-6120.

Kaveh, A. and Farhoudi, N. (2013), "A new optimization method:

dolphin echolocation", *Adv. Eng. Softw.*, **59**, 53-70.
Kaveh, A. and Maniat, M. (2015), "Damage detection based on MCSS and PSO using modal data", *Smart Struct. Syst.*, **15**(5), 1253-1270.
Kaveh, A. and Talatahari, S. (2010), "A novel heuristic optimization method: charged system search", *Acta Mechanica*, **213**(3-4), 267-289.
Kaveh, A. and Zolghadr, A. (2015), "An improved CSS for damage detection of truss structures using changes in natural frequencies and mode shapes", *Adv. Eng. Softw.*, **80**, 93-100.
Maity, D. and Tripathy, R.R. (2005), "Damage assessment of structures from changes in natural frequencies using genetic algorithm", *Struct. Eng. Mech.*, **19**(1), 21-42.
Manoharan, R., Vasudevan, R. and Jeevanantham, A.K. (2015), "Optimal layout of a partially treated laminated composite magnetorheological fluid sandwich plate", *Smart Struct. Syst.*, **16**(6), 1023-1047.
Messina, A., Williams, E.J. and Contursi, T. (1998), "Structural damage detection by a sensitivity and statistical-based method", *J. Sound Vib.*, **216**(5), 791-808.
Moradi, S., Razi, P. and Fatahi, L. (2011), "On the application of bees algorithm to the problem of crack detection of beam-type structures", *Comput. Struct.*, **89**(23), 2169-2175.
Nobahari, M. and Seyedpoor, S.M. (2011), "Structural damage detection using an efficient correlation-based index and a modified genetic algorithm", *Math. Comput. Model.*, **53**(9), 1798-1809.
Perera, R. and Torres, R. (2006), "Structural damage detection via modal data with genetic algorithms", *J. Struct. Eng.*, **132**(9), 1491-1501.
Rashedi, E., Nezamabadi-Pour, H. and Saryazdi, S. (2009), "GSA: a gravitational search algorithm", *Inform. Sci.*, **179**(13), 2232-2248.
Sahoo, B. and Maity, D. (2007), "Damage assessment of structures using hybrid neuro-genetic algorithm", *Appl. Soft Comput.*, **7**(1), 89-104.
Sandesh, S. and Shankar, K. (2010), "Application of a hybrid of particle swarm and genetic algorithm for structural damage detection", *Inverse Problem. Sci. Eng.*, **18**(7), 997-1021.
Seyedpoor, S.M. (2012), "A two stage method for structural damage detection using a modal strain energy based index and particle swarm optimization", *Int. J. Non-Lin. Mech.*, **47**(1), 1-8.
Seyedpoor, S.M. and Montazer, M. (2016), "A two-stage damage detection method for truss structures using a modal residual vector based indicator and differential evolution algorithm", *Smart Struct. Syst.*, **17**(2), 347-361.
Shirazi, M.N., Mollamahmoudi, H. and Seyedpoor, S.M. (2014), "Structural damage identification using an adaptive multi-stage optimization method based on a modified particle swarm algorithm", *J. Optimiz. Theory Appl.*, **160**(3), 1009-1019.
Wang, H. and Ohmori, H. (2013), "Elasto-plastic analysis based truss optimization using Genetic Algorithm", *Eng. Struct.*, **50**, 1-12.
Xiang, J. and Liang, M. (2012), "A two-step approach to multi-damage detection for plate structures", *Eng. Fract. Mech.*, **91**, 73-86.

CC